THE JOURNAL OF PHYSICAL CHEMISTRY B

Article

pubs.acs.org/JPCB

Unraveling the Benzocaine–Receptor Interaction at Molecular Level Using Mass-Resolved Spectroscopy

Edurne Aguado,[†] Iker León,[†] Judith Millán,[‡] Emilio J. Cocinero,[†] Sander Jaeqx,[§] Anouk M. Rijs,[§] Alberto Lesarri,[∥] and José A. Fernández*[,†]

[†]Departamento de Química Física, Facultad de Ciencia y Tecnología, Universidad del País Vasco (UPV/EHU), B° Sarriena s/n, 48940 Leioa, Spain

[‡]Departamento de Química, Facultad de Ciencias, Estudios Agroalimentarios e Informática, Universidad de La Rioja, Madre de Dios, 51, 26006 Logroño, Spain

[§]Radboud University Nijmegen, Institute for Molecules and Materials, FELIX Facility, Toernooiveld 7, 6525 ED Nijmegen, The Netherlands

[∥]Departamento de Química Física y Química Inorgánica, Facultad de Ciencias, Universidad de Valladolid, E-47011 Valladolid, Spain

Supporting Information

ABSTRACT: The benzocaine–toluene cluster has been used as a model system to mimic the interaction between the local anesthetic benzocaine and the phenylalanine residue in Na^+ channels. The cluster was generated in a supersonic expansion of benzocaine and toluene in helium. Using a combination of mass-resolved laser-based experimental techniques and computational methods, the complex was fully characterized, finding four conformational isomers in which the molecules are bound through N–H···π and π···π weak hydrogen bonds. The structures of the detected isomers closely resemble those predicted for benzocaine in the inner pore of the ion channels, giving experimental support to previously reported molecular chemistry models.

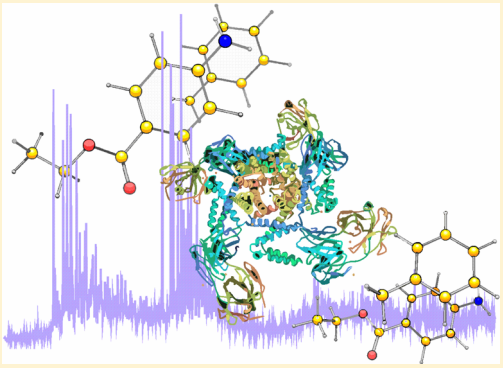

INTRODUCTION

Cation channels are membrane proteins that allow the interchange of positive ions between the cell and its surrounding medium. They are regulated using agonist (opening) or antagonist (closing) molecules. Some ion channels, named voltage-gated ion channels, such as the Na^+ neuron channels which are responsible for propagation of the electric signal along the neuron's axon, have additional voltage sensors that trigger the opening of the pore when a membrane depolarization occurs. Together with the K^+ and the Ca^{2+} voltage-gated channels, they are present in all kingdoms of life,[1] and are a common target for many drugs, such as pain relievers (mainly local anesthetics) and antiarrhythmic pharmaceuticals.[2]

Despite the importance of the ion channels, little is known about how they work at the molecular level. Membrane proteins generally cannot be crystallized, so only a few X-ray structures are reported so far, mostly cocrystallized with soluble proteins.[1,3−6] The lack of experimental data on the receptor structure at atomic resolution seriously hampers understanding their function and has been recognized as "the main stumbling block to further progress".[7] Obtaining accurate data on the interaction mechanism of agonist and antagonist molecules (including drugs) with the channels is thus a priority to understand the docking process that controls opening or closing of the pore.

Local anesthetics exhibit different affinities[8−10] for the receptor depending on the channel state (open, close resting state, or inactive[11]). Li et al.[12] demonstrated that, by replacing two amino acids, a tyrosine (Y1717) residue and a phenylalanine (F1710) residue, a strong modulation in the affinity of the voltage-gated Na^+ channels from a mammalian brain is achieved. Moreover, a single phenylalanine in domain IV, S6 (F1759), seems to be critical for the affinity of local anesthetics to $Na_v1.5$ and $Na_v1.4$ channels,[10,13] while F1764 and Y1771 play the same role in $Na_v1.2$.[14] Thus, independently of the type or subtype of ion channel, a single residue (or two in some channels) close to the narrowest part of the pore seems to be determinant for the action of the local anesthetics to take place.

In other experiments, the affinity of several local anesthetics for docking into the selectivity filter (the narrow part of the channel which allows only the entrance of ions of the correct size) was determined. Lipkind and Fozzard[10] built a model of an ion channel using crystallographic data and determined that local anesthetics were able to dock with the F1579 residue in its open state. However, only benzocaine was able to dock while the channel was in its closed configuration, stabilizing such a

Received: July 12, 2013
Revised: September 24, 2013
Published: September 24, 2013

configuration and preventing its aperture. In a different study, Hanck et al. confirmed that the ability of benzocaine to dock while the channel is in its closed state is the origin of its antiarrhythmic properties.[13] The authors proposed a direct N−H···π interaction between benzocaine and the F1579 residue at the selectivity filter. Benzocaine (Scheme 1) is thus a suitable

Scheme 1. Benzocaine (*p*-Amino Ethyl Benzoate), Phenylalanine, and Toluene

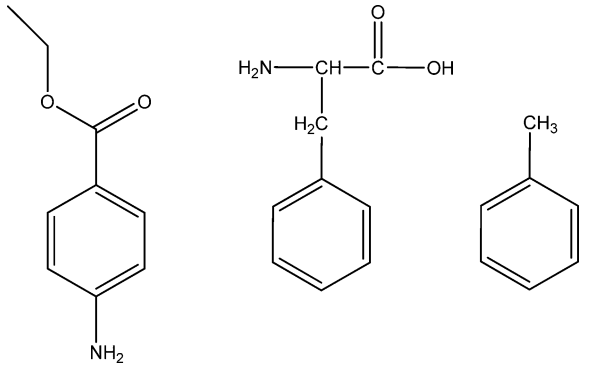

anesthetic to examine the interactions with the selectivity filter of the Na^+ channels at a molecular level. More specifically, a molecular cluster formed by benzocaine and a putative binding partner, like phenylalanine, can be useful to isolate the local association in the binding pocket, extracting the physical aspects of this interaction. Benzocaine presents several groups that may compete for interactions with the aromatic residue. At first glance, a strong $\pi\cdots\pi$ interaction between the aromatic rings of both molecules might be the best candidate, since these links are often found in biological systems, such as DNA,[15] protein−protein,[16] and protein−DNA.[17] However, the amino group of benzocaine is also able to establish N−H···π hydrogen bonds which may be of comparable strength. Therefore, several orientations of benzocaine are possible inside the pore.

Since the benzocaine−phenylalanine interactions at the binding site are expected to proceed through the side chain of the amino acid residue, we decided to examine the intermolecular aggregate formed by benzocaine and toluene. This is an accepted reductionist approach, successfully employed in many previous works on the interaction between organic molecules and amino acids, as the rest of the amino acid is separated enough from the aromatic ring so as not to modify its interaction with other molecules.[18]

Benzocaine−toluene clusters can be formed using supersonic expansions, which create the cold and collision-free conditions required to freeze the clusters in a time interval that can be probed with high-resolution pulsed laser techniques. Sensitive detection can be accomplished using time-of-flight mass spectrometry, which is combined with laser-based excitation spectroscopic techniques, providing vibronic and pure vibrational information. The experimental data obtained will be compared with predictions from high level quantum chemical calculations. This methodology allows obtaining the structure of the experimentally observed clusters, as demonstrated in previous studies on the noncovalent interactions of small molecules,[19−24] proteins,[25−30] sugars,[31−35] DNA bases,[36−41] and drugs.[42−46]

Finally, a comparison between the results from this work with the predictions from previous studies on the interactions of benzocaine in the selectivity filter is offered.

METHODS

Experimental Section. The experimental methodology was previously described,[42,47] and therefore, only the most relevant details are discussed here. Benzocaine (Sigma-Aldrich, 99%) was heated in an oven at ∼140 °C, while toluene was placed in a different compartment at room temperature. The mixture of both chemicals was seeded in He/Ar at typical pressures of 2−5 bar. The resulting mixture was expanded using a pulsed valve (Jordan Inc.) maintained at 70 °C, inside the ionization chamber of a time-of-flight spectrometer (Jordan Inc.), where it was interrogated by up to three lasers. Due to the temperature difference between the valve and oven, some condensation takes place, but enough vapor pressure was still obtained to carry out the experiment.

Two-color REMPI (resonance-enhanced multiphoton ionization) was carried out tuning the ionization laser close to the ionization threshold of the species of interest to avoid fragmentation. Likewise, a two-color detection scheme was used in UV/UV hole burning experiments. Typical delays of 200−800 ns were employed between the "burning" laser and the two lasers used for detection. The "burning" laser was fired at 5 Hz, while the laser couple used for detection was fired at 10 Hz to carry out an active subtraction, improving the S/N (signal-to-noise) ratio. The laser energy was kept around 100 μJ/pulse for the pump laser and around 1 mJ/pulse for the probe.

A similar scheme was used in IR/UV experiments, although replacing the UV "burning" laser by an IR laser (Fine Adjustment Inc.), which generates tunable radiation in the ∼3000−4000 cm^{-1} region. Around 0.5−0.8 μJ/pulse were obtained in the 3200−3800 cm^{-1} region. Below 3200 cm^{-1}, the IR laser energy drops very fast.

The spectroscopy in the 500−1800 cm^{-1} region was carried out in the free-electron laser facility FELIX. The setup used for these experiments is described in more detail elsewhere.[48] Briefly, the molecular beam produced by a Jordan valve is skimmed before entering the differentially pumped reflector time-of-flight mass spectrometer (Jordan). Here, the benzocaine−toluene clusters interact with the UV beam and IR laser beams. The IR absorption spectra are recorded in the frequency range between 500 and 1800 cm^{-1} showing the amide I, amide II, and fingerprint region. FELIX produces pulses with a pulse duration of the macropulse of about 6 μs, pulse energies of 100 mJ, and a spectral line width of typically 0.5% of the frequency. Both the UV laser and the molecular beam are running at 10 Hz, while FELIX is running at 5 Hz. In order to minimize signal fluctuations due to long-time drifts in the UV laser power or source conditions, a normalized IR spectrum is obtained by recording alternating IR-off and IR-on signals. Moreover, the IR spectra are corrected for the intensity variations of the IR power over the complete wavelength range.

Computational. A detailed description of the calculation procedure can be found elsewhere.[43,45] In summary, a thorough exploration of the conformational landscape of benzocaine−toluene was carried out using molecular mechanics (MMFFs force field[49−51]). More than 60 structures were selected for further optimization using density functional theory (M05-2X, M06-2X) and *ab initio* methods (MP2) with several basis sets (6-31+G(d), 6-311+G(d,p), 6-311++G(d,p)). For the sake of brevity, only the results at the M06-2X/6-311++G(d,p) level are presented here, as they are the ones that better reproduce the experimental values. All the structures were subjected to

dx.doi.org/10.1021/jp4068944 | J. Phys. Chem. B 2013, 117, 13472−13480

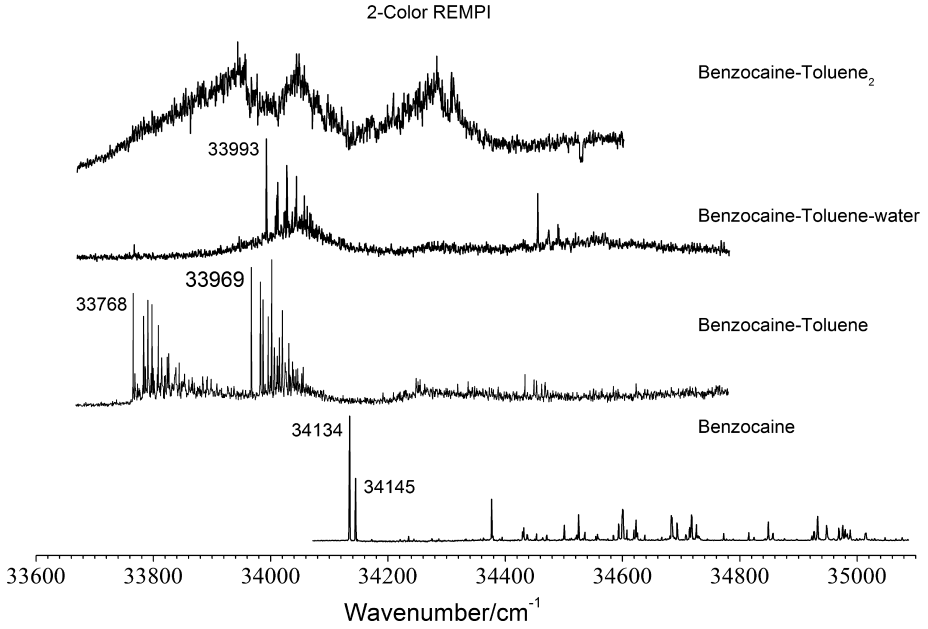

Figure 1. Comparison between the two-color spectrum of benzocaine and of its clusters with toluene, toluene−water, and toluene dimer.

normal-mode analysis to ensure that they are true minima structures, and the zero-point energy (ZPE) value obtained in such calculations was used to correct the energy values. An estimation of the BSSE was done using the counterpoise procedure,[52] and the value was used to produce BSSE-corrected energy values. All calculations were performed using Gaussian 09.[53]

RESULTS

Benzocaine has two conformers, *trans* and *gauche*, depending on the orientation of the ethyl group.[54,55] In the *trans* conformation, the heavy-atom skeleton is planar, while the terminal methyl group is nearly perpendicular to the plane of the ring in the *gauche* conformation. The lowest energy *gauche* structure is only less than 2 kJ/mol above the *trans* global minimum, and the barrier separating both conformers is low enough to allow population transfer from the *gauche* to the *trans* conformer if (heavier) Ar carrier gas is used instead of He in the supersonic expansion.[42,56] Figure 1 shows a comparison between the two-color spectrum of benzocaine, benzocaine−toluene, benzocaine−toluene−water, and benzocaine−toluene$_2$. The 0_0^0 transitions of the two conformers of benzocaine are clearly visible at 34134 and 34145 cm^{-1}, respectively. Formation of the benzocaine−toluene cluster results in a 366 cm^{-1} red shift of the 0_0^0 transition and in the appearance of a number of vibronic intermolecular modes. As it will be shown below, the spectrum contains a contribution from at least four different isomers.

Benzocaine is a hygroscopic molecule, and therefore, the samples always contain a certain amount of water,[57] which is large enough to allow formation of the benzocaine−toluene−water heterotrimer, as is shown in Figure 1. Therefore, fragmentation was avoided by careful tuning of the experimental conditions. Special care was taken to avoid fragmentation from other higher-order clusters present in the expansion, such as benzocaine−toluene$_2$, which could complicate the interpretation of the spectrum.

The number of conformational isomers is determined by using UV/UV hole burning spectroscopy. Figure 2 collects the

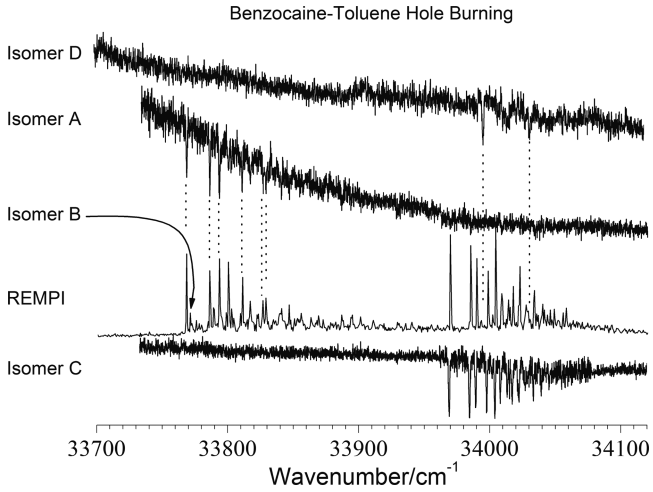

Figure 2. UV/UV hole burning traces recorded tuning the two-color detection to the transitions at 33768, 33969, and 33993 cm^{-1}. A fourth isomer with 0_0^0 transition at 33771 cm^{-1} was detected. This transition did not appear in the hole burning traces of the other isomers.

hole burning traces of the benzocaine−toluene cluster recorded by probing the transitions at 33768, 33969, and 33993 cm^{-1}, which correspond to three different isomers (A, C, and D). The hole burn trace of the fourth isomer B, with its 0_0^0 transition at 33771 cm^{-1}, could not be recorded due to its low signal strength. All four isomers appear to the red of the origin band of the bare molecule, pointing to a direct interaction with the electronic cloud of benzocaine. Such interactions are usually due to dispersive forces; excitation of the electronic cloud increases its volume and therefore its polarizability, reinforcing such kind of interactions.[58] Also, the position of the 0_0^0 transitions of the four detected isomers, i.e., the division in two sets of absorptions, seems to indicate that they correspond to two types of interactions. One set of isomers is expected to be based on a *trans*-benzocaine core, while the other contains a *gauche*-benzocaine core.

dx.doi.org/10.1021/jp4068944 | J. Phys. Chem. B 2013, 117, 13472−13480

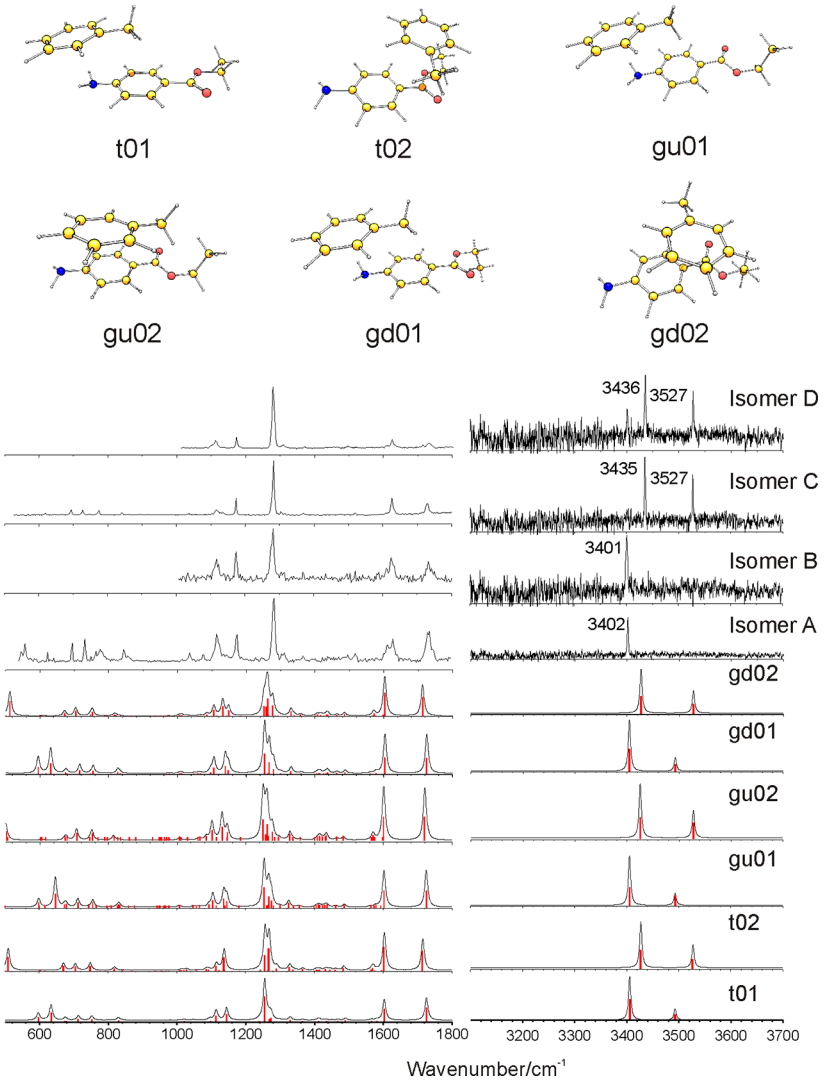

Figure 3. Comparison between the IR/UV double resonance spectra obtained for the four benzocaine−toluene isomers (traces A−D) and the simulated spectra for some of the calculated structures. A 0.9482 scaling factor was used to account for anharmonicity, based on the comparison between experimental and calculated frequencies for benzocaine. All the structures and simulated spectra can be found in the Supporting Information.

Additional experimental evidence was collected to carry out a more precise assignment. The IR/UV hole burning spectra of the four isomers were recorded in both the fingerprint/amide I/II region and the N−H stretching region (see Figure 3). As can be seen in this figure, slight differences between the spectra of the four isomers were observed in the fingerprint region, especially in the 600−800 cm^{-1} interval. Furthermore, the spectra in the N−H stretching region of isomers A and B are significantly different from those of isomers C and D; a single peak is detected for the former, while two peaks (slightly shifted to the blue) are found for the latter.

Figure 3 also shows the spectra predicted for some of the calculated structures. Using the above-described procedure, 123 structures grouped in 44 families were found, in which three types of interactions are present: N−H···π, π···π, and the interaction between the ester group and toluene's aromatic cloud (abbreviated as C═O···π). In addition, attending to the orientation of the ester group, benzocaine can adopt the plane-symmetric *trans* (structures labeled as t*n*, where *n* = 01, 02, ... starting with the most stable structure) or *gauche* conformations. Due to the symmetry break introduced in *gauche*-benzocaine by the orientation of the ethyl group, those isomers in which the two rings are parallel can be divided into *gauche up*, if the ethyl group is on the same side of the ring as the toluene (structures gu*n*, *n* = 01, 02, ...), and *gauche down* (gd*n*, *n* = 01, 02, ...), if the ethyl group and the toluene are on opposite sides of the benzocaine ring. In the structures in which the toluene interacts with the ester group, the difference *up/down* is lost and then the structures are labeled as g*n* (*n* = 01, 02, ...). Figure 4 shows some representative calculated structures, while the complete collection can be found in Figure S1 (Supporting Information). Because of the size of the cluster and the better agreement with the experimental data, we only report here the M06-2X/6-311++G(d,p) results.

The global minimum (t01) corresponds to a *trans*-based structure with N−H···π and C−H···π interactions, but the *gauche*-based analogues are less than 2 kJ/mol higher in energy (gu01 and gd01) and therefore they may be populated at the temperature of the expansion. The structures with π···π interactions (t02, gu02, gd02, ...) are also close in energy, although in some of such structures, the toluene is shifted toward the ester substituent. Finally, the less stable structures

dx.doi.org/10.1021/jp4068944 | J. Phys. Chem. B 2013, 117, 13472−13480

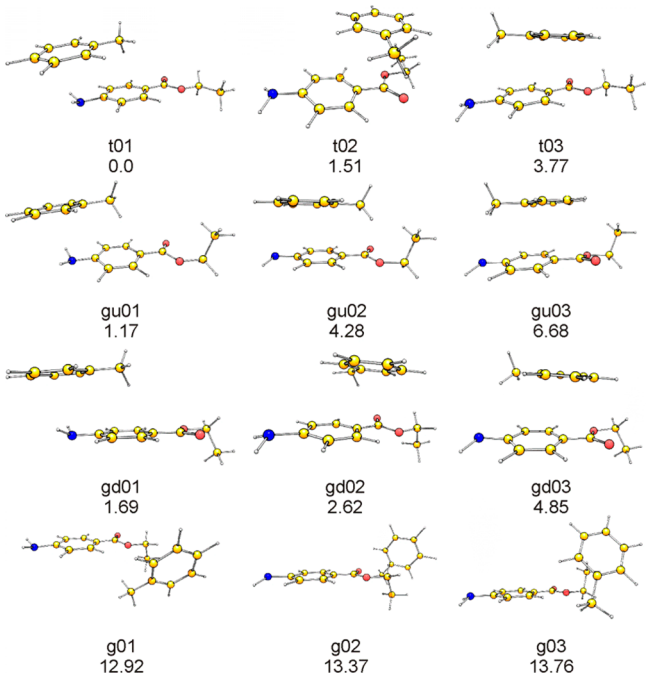

Figure 4. A selection of the benzocaine−toluene structures calculated at the M06-2X/6311++G(d,p) level, together with their relative stability in kJ/mol. The complete set of structures can be found in Figure S1 (Supporting Information).

are those in which the toluene occupies a position in one side of the ester group (g01, g02, t14, ...) which appears >11 kJ/mol above the global minimum.

No simulated spectrum was able to reproduce the appearance of a single N−H stretch in the 3200−3600 cm^{-1} region of isomers A and B in Figure 3. However, N−H···π interactions are predicted to induce a strong reduction in the intensity of the NH_2 asymmetric stretch. Furthermore, they are expected to exhibit a slightly larger red shift with respect to the bare molecule N−H stretches than those structures with π···π interactions. The bare molecule N−H stretches appear at 3435 and 3527 cm^{-1} in *trans*-benzocaine and at 3438 and 3531 cm^{-1} in *gauche*-benzocaine.[42] According to these characteristics, the experimental spectra of isomers A and B should correspond to species in which there is an N−H···π interaction, while isomers C and D are due to species with π···π interactions. In the absence of other evidence, the higher intensity of the spectra of isomers A and C seems to indicate that they are based on a *trans*-benzocaine core, while benzocaine adopts a *gauche* conformation in the other two isomers and its lower intensity would be due to the lower population of the *gauche* conformer in the expansion.

Such an assignment is reinforced by the comparison between experimental and calculated spectra in the 600−800 cm^{-1} range. Those structures with N−H···π interactions (t01, gu01, and gd01 in Figure 3) present stronger bands in the 800−600 cm^{-1} region than those structures with π···π interactions (t02, gu02, and gd02 in Figure 3). Likewise, the bands on the spectrum of isomer A in such a region are stronger than those on the spectrum of isomer C. Unfortunately, not enough beamline time was allocated to record all four spectra in the 400−800 cm^{-1} region.

In order to find further evidence to confirm the assignment proposed above, a TD-DFT study was carried out. Although such calculations usually yield excitation energies several thousand cm^{-1} higher than the experimental values, they are able to predict the correct energetic order.[59] Figure 5 shows a comparison between the $S_1 \leftarrow S_0$ values estimated for some selected isomers and the experimental spectrum. The red sticks correspond to the three isomers with N−H···π interactions, the green sticks correspond to isomers with π···π interactions, and those with interactions between the toluene aromatic ring and the ester substituent appear in blue. Clearly, the calculations predict that the 0_0^0 transitions of those isomers with N−H···π interactions will appear to the red and with lower intensities than the isomers with π···π interactions, in good agreement with the assignments based on the analysis of the IR/UV spectra.

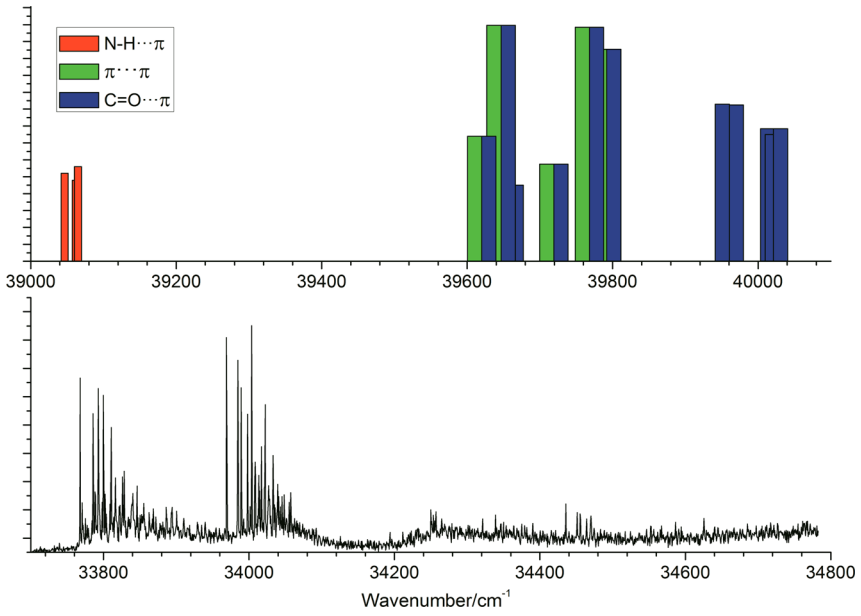

Figure 5. TD-DFT estimation of the excitation energy for several calculated benzocaine−toluene isomers. The two-color REMPI spectrum is also shown for comparison.

dx.doi.org/10.1021/jp4068944 | J. Phys. Chem. B 2013, 117, 13472−13480

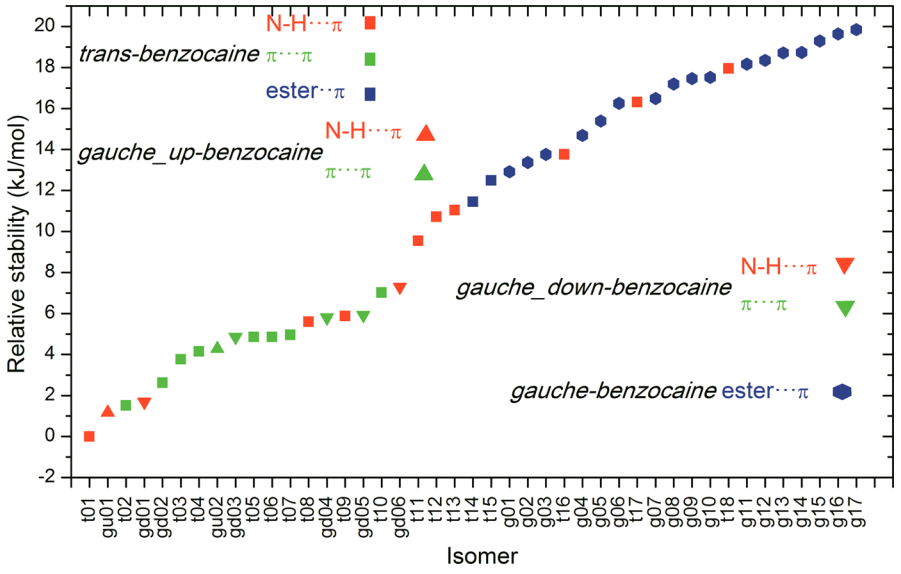

Figure 6. Conformational distribution of the calculated benzocaine−toluene clusters.

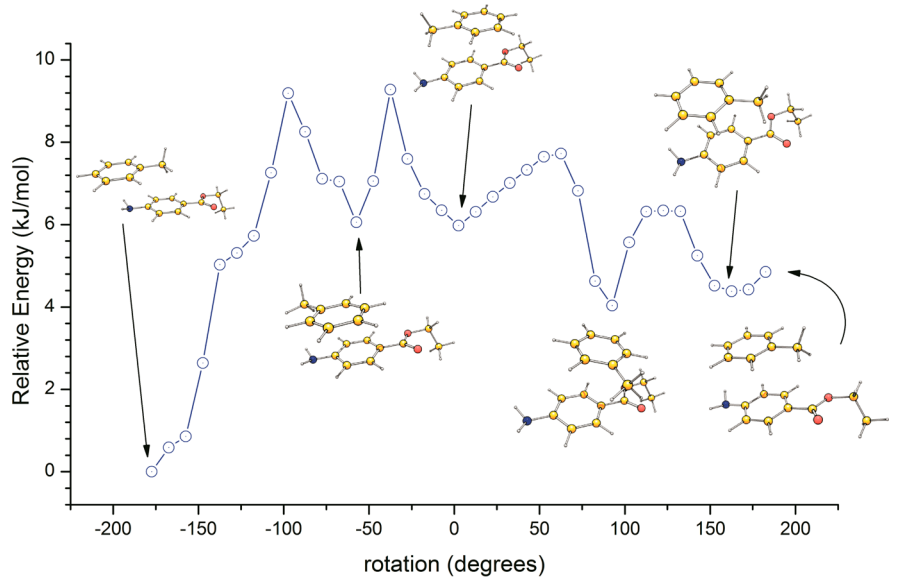

Figure 7. Energy path obtained rotating the toluene molecule above the benzocaine, using isomer gd01 as a starting structure.

A final test on the assignment was carried out comparing the ionization thresholds determined in a two-color REMPI experiment (Figure S3 and Table S2 of the Supporting Information) with those estimated from the energy difference between D_0^+ and S_0 structures of the calculated isomers. The calculations predict that the isomers with N−H···π interactions will have an ionization threshold ∼600 cm^{-1} lower than those with stacking interactions, reinforcing the assignments. However, they also predict ionization thresholds ∼300 cm^{-1} lower for the *gauche*-based conformers than for those containing a *trans*-benzocaine core, which is against the proposed assignment. Therefore, the comparison of ionization thresholds was not conclusive.

DISCUSSION

Conformational Energies. Four isomers of the benzocaine−toluene cluster were detected in a jet expansion: two of them contain a combination of N−H···π and C−H···π interactions and the other two with stacking interactions. All four detected isomers are within a 3 kJ/mol window, which fits very well with the population expected at 340 K, the temperature at which the valve is maintained prior to the expansion.

The analysis of the conformational distribution gives some hints on the relative importance of the different interactions. For example, the most stable isomer, t01, presents N−H···π and C−H···π interactions. Removal of the C−H···π interaction (red squares in Figure 6) by rotation of the toluene over the amino group results in a >5 kJ/mol loss of stability (isomer t08). The estimated dissociation energy of t01 is 29 kJ/mol, and therefore, the N−H···π clearly is the dominant interaction in the formation of isomer t01.

On the other hand, t02, the most stable stacked cluster (green squares), is less than 2 kJ/mol above the global minimum. Taking into account the size of the system and the smooth potential energy surfaces usually found for staking interactions,[60−62] one would expect the less stable structures to collapse into the most stable ones during the cooling process.

dx.doi.org/10.1021/jp4068944 | J. Phys. Chem. B 2013, 117, 13472−13480

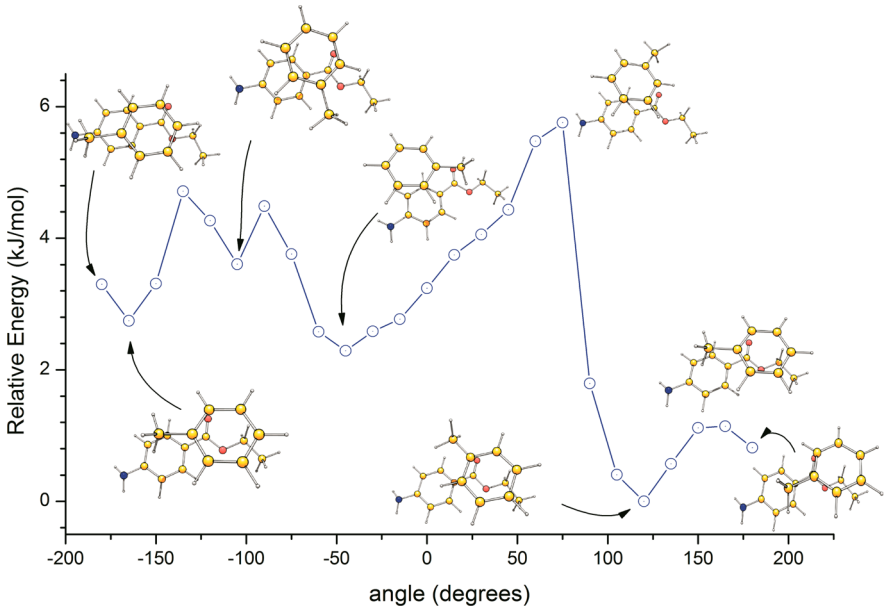

Figure 8. Energy path obtained rotating the toluene molecule above the benzocaine, using isomer t02 as a starting structure.

In order to map the potential energy surface and to find the possible paths connecting the different minima, several calculations were performed: starting from the gd01 structure, the toluene molecule was rotated above the benzocaine, while the rest of the degrees of freedom were relaxed (Figure 7). The same calculation but taking t03 as the starting point resulted in the energy path in Figure 8, while starting from gu02, Figure S4 (Supporting Information) is obtained. Calculation of several additional reaction paths was also attempted but serious convergence problems were encountered, which made it impossible to complete the calculations.

Inspection of the energy paths leads to several conclusions; first, a 360° rotation does not result in the initial structure, and therefore, several more degrees of freedom must be included in the study to obtain a good description of the paths connecting the different minima. Second, most of the barriers are below 4 kJ/mol and therefore could be surmounted during the cooling process. This is consistent with the commonly accepted description of flat and smooth potential energy surfaces for the interaction between aromatic rings. Thus, if two isomers with N−H···π and stacking interactions, respectively, are still detected, it must be because the sudden cooling process is faster than the population migration process between minima.

Comparison with an Ionic Channel Model. The existence of a direct interaction between benzocaine and a phenylalanine residue in the Na^+ channel has been previously established. Hanck et al. built a theoretical model for the interaction of benzocaine and lidocaine with the $Na_v1.5$ channel using the structure of KcSA,[13] which can now be tested against the observations for the benzocaine−toluene cluster. According to the authors, the antagonist activity of benzocaine could be explained by a direct N−H···π interaction of benzocaine with the phenyl ring of F1579, which exists when the pore is either in the open or closed state. The structure suggested in Hanck's work very much resembles that of isomer t01, especially when the pore is open. The small differences between the position of benzocaine in the pore reported in ref 13 and the structure of isomer t01 are probably due to secondary interactions between benzocaine and other amino acid residues. In particular, the interactions with F1464 and Y1766 are similar to those observed in the g0n isomers calculated in this work, and therefore, one would expect them to be significantly less important than the main interaction with F1579. One must keep in mind that substitution of F1579 with non-aromatic amino acids results in an important decrease in the high-affinity local anesthetic block.[13] Also, the low barriers connecting the many isomers found for benzocaine−toluene translate in the bio system into a low-barrier path that allows benzocaine to achieve its optimal blocking position below the selectivity filter of the channel.

Furthermore, the proposed structure would explain the difference in affinity between benzocaine and those local anesthetics with charged amines under physiological conditions, because the stronger N^+−H···π interaction in the latter changes the optimal position in the filter.

CONCLUSIONS

In this work, benzocaine−toluene clusters were formed using supersonic expansions. Using several laser spectroscopic techniques, the two-color REMPI spectrum of the complex was obtained. The contributions of at least four conformational isomers to the spectrum were revealed, using UV/UV hole burning spectroscopy, while their mass-resolved IR spectra were obtained using IR-UV double resonance techniques. Comparison of the experimental data and the estimated transition and ionization energy values with those predicted at M06-2X/6-311++G(d,p) allowed us to conclude that two of the isomers present N−H···π and C−H···π interactions, while the other two are based on stacked interactions. The most stable N−H···π conformations are consistent with the theoretical predictions for the large-scale interactions of benzocaine docked with the $Na_v1.5$ channel. The channel models thus receive experimental validation through the analysis of the local interactions present in the structure of benzocaine−toluene. The analysis of other clusters involving benzocaine and other binding partners is in progress to achieve a detailed understanding of the non-covalent forces acting in the large protein receptors.

dx.doi.org/10.1021/jp4068944 | J. Phys. Chem. B 2013, 117, 13472−13480

■ ASSOCIATED CONTENT

Supporting Information

All calculated structures, predicted IR spectra, and computed relative stabilities of the species studied in this work, additional reaction paths, and ionization thresholds. This material is available free of charge via the Internet at http://pubs.acs.org.

■ AUTHOR INFORMATION

Corresponding Author

*E-mail: josea.fernandez@ehu.es. Fax: + 34 94 601 35 00. Phone: + 34 94 601 5387. Web site: https://sites.google.com/site/gesemupv/.

Notes

The authors declare no competing financial interest.

■ ACKNOWLEDGMENTS

The research leading to these results has received funding from Spanish Ministry of Science and Innovation-MICINN (CTQ2012-39132 and CTQ2011-22923) and from UPV/EHU (UFI 11/23). I.L. thanks the GV for pre- and post-doctoral fellowships, and E.J.C. thanks the Spanish Ministry (MICINN) for a "Ramón y Cajal" Contract. Computational resources from the SGI/IZO-SGIker and from i2BASQUE academic network were used for this work. Technical and human support provided by the Laser Facility of the SGIKER (UPV/EHU, MICINN, GV/EJ, ESF) is also gratefully acknowledged. We gratefully acknowledge the expert assistance of the FELIX group. This work is part of the research program of FOM, which is financially supported by the Nederlandse Organisatie voor Wetenschappelijk Onderzoek (NWO).

■ REFERENCES

(1) Long, S. B.; Campbell, E. B.; MacKinnon, R. Crystal Structure of a Mammalian Voltage-Dependent Shaker Family K+ Channel. *Science* **2005**, *309*, 897−903.

(2) Brunton, L. L.; Lazo, J. S.; Parker, K. L. *Goodman & Gilman's The Pharmacological Basis of Therapeutics*, 11th ed.; McGraw Hill: New York, 2006.

(3) Nury, H.; Van Renterghem, C.; Weng, Y.; Tran, A.; Baaden, M.; Dufresne, V.; Changeux, J. P.; Sonner, J. M.; Delarue, M.; Corringer, P. J. X-Ray Structures of General Anaesthetics Bound to a Pentameric Ligand-Gated Ion Channel. *Nature* **2011**, *469*, 428−431.

(4) Bocquet, N.; Nury, H.; Baaden, M.; Le Poupon, C.; Changeux, J. P.; Delarue, M.; Corringer, P. J. X-Ray Structure of a Pentameric Ligand-Gated Ion Channel in an Apparently Open Conformation. *Nature* **2009**, *457*, 111−114.

(5) Jiang, Y.; Lee, A.; Chen, J.; Cadene, M.; Chait, B. T.; MacKinnon, R. Crystal Structure And Mechanism of a Calcium-Gated Potassium Channel. *Nature* **2002**, *417*, 515−522.

(6) Payandeh, J.; Scheuer, T.; Zheng, N.; Catterall, W. A. The Crystal Structure of a Voltage-Gated Sodium Channel. *Nature* **2011**, *475*, 353−358.

(7) Chau, P. L. New Insights Into The Molecular Mechanisms of General Anaesthetics. *Br. J. Pharmacol.* **2010**, *161*, 288−307.

(8) Hille, B. Local Anesthetics: Hydrophilic And Hydrophobic Pathways For The Drug-Receptor Reaction. *J. Gen. Physiol.* **1977**, *69*, 497−515.

(9) Liu, H.; Atkins, J.; Kass, R. S. Common Molecular Determinants of Flecainide and Lidocaine Block of Heart Na+ Channels: Evidence from Experiments with Neutral and Quaternary Flecainide Analogues. *J. Gen. Physiol.* **2003**, *121*, 199−214.

(10) Lipkind, G. M.; Fozzard, H. A. Molecular Modeling of Local Anesthetic Drug Binding by Voltage-Gated Sodium Channels. *Mol. Pharmacol.* **2005**, *68*, 1611−1622.

(11) Hille, B. *Ion Channels of Excitable Membranes*, 3rd ed.; Sinauer Associates Inc.: Sunderland, MA, 1992.

(12) Li, H. L.; Galue, A.; Meadows, L.; Ragsdale, D. S. A Molecular Basis for the Different Local Anesthetic Affinities of Resting Versus Open and Inactivated States of the Sodium Channel. *Mol. Pharmacol.* **1999**, *55*, 134−141.

(13) Hanck, D. A.; Nikitina, E.; McNulty, M. M.; Fozzard, H. A.; Lipkind, G. M.; Sheets, M. F. Using Lidocaine and Benzocaine to Link Sodium Channel Molecular Conformations to State-Dependent Antiarrhythmic Drug Affinity. *Circ. Res.* **2009**, *105*, 492−499.

(14) Ragsdale, D. S.; McPhee, J. C.; Scheuer, T.; Catterall, W. A. Molecular Determinants of State-Dependent Block of Na^+ Channels By Local Anesthetics. *Science* **1994**, *265*, 1724−1728.

(15) Stephenson, W.; Asare-Okai, P. N.; Chen, A. A.; Keller, S.; Santiago, R.; Tenenbaum, S.; Garcia, A. E.; Fabris, D.; Li, P. T. The Essential Role of Stacking Adenines in a Two-Base-Pair RNA Kissing Complex. *J. Am. Chem. Soc.* **2013**, *135*, 5602−5611.

(16) Lanzarotti, E.; Biekofsky, R. R.; Estrin, D. A.; Marti, M. A.; Turjanski, A. G. Aromatic-Aromatic Interactions in Proteins: Beyond the Dimer. *J. Chem. Inf. Model.* **2011**, *51*, 1623−1633.

(17) Blakaj, D. M.; McConnell, K. J.; Beveridge, D. L.; Baranger, A. M. Molecular Dynamics and Thermodynamics of Protein-RNA Interactions: Mutation of a Conserved Aromatic Residue Modifies Stacking Interactions and Structural Adaptation in the U1A-Stem Loop 2 RNA Complex. *J. Am. Chem. Soc.* **2001**, *123*, 2548−2551.

(18) de Vries, M. S.; Hobza, P. Gas-Phase spectroscoyp of biomolecular building blocks. *Annu. Rev. Phys. Chem.* **2007**, *58*, 585−612.

(19) Hu, Y. J.; Fu, H. B.; Bernstein, E. R. IR Plus Vacuum Ultraviolet Spectroscopy of Neutral And Ionic Organic Acid Molecules and Clusters: Acetic Acid. *J. Chem. Phys.* **2006**, *125*, 184308.

(20) Hu, Y. J.; Fu, H. B.; Bernstein, E. R. IR Plus Vacuum Ultraviolet Spectroscopy of Neutral and Ionic Organic Acid Monomers and Clusters: Propanoic Acid. *J. Chem. Phys.* **2006**, *125*, 184309.

(21) Hu, Y. J.; Fu, H. B.; Bernstein, E. R. Infrared Plus Vacuum Ultraviolet Spectroscopy of Neutral and Ionic Ethanol Monomers and Clusters. *J. Chem. Phys.* **2006**, *125*, 154305.

(22) Clarkson, J. R.; Baquero, E.; Shubert, V. A.; Myshakin, E. M.; Jordan, K. D.; Zwier, T. S. Laser-Initiated Shuttling of a Water Molecule Between H-Bonding Sites. *Science* **2005**, *307*, 1443−1446.

(23) Dian, B. C.; Clarkson, J. R.; Zwier, T. S. Direct Measurement of Energy Thresholds to Conformational Isomerization in Tryptamine. *Science* **2004**, *303*, 1169−1173.

(24) Zwier, T. Laser Spectroscopy of Jet-Cooled Biomolecules and Their Water-Containing Clusters: Water Bridges and Molecular Conformation. *J. Phys. Chem. A* **2001**, *105*, 8827−8839.

(25) Baquero, E. E.; James, W. H.; Choi, S. H.; Gellman, S. H.; Zwier, T. S. Single-Conformation Ultraviolet and Infrared Spectroscopy of Model Synthetic Foldamers: Beta-Peptides Ac-beta(3)-hPhe-NHMe and Ac-beta(3)-hTyr-NHMe. *J. Am. Chem. Soc.* **2008**, *130*, 4784−4794.

(26) Toroz, D.; Van Mourik, T. The Structure of the Gas-Phase Tyrosine-Glycine Dipeptide. *Mol. Phys.* **2006**, *104*, 559−570.

(27) Bakker, J.; Plutzer, C.; Hunig, I.; Haber, T.; Compagnon, I.; von Helden, G.; Meijer, G.; Kleinermanns, K. Folding Structures of Isolated Peptides as Revealed by Gas-Phase Mid-Infrared Spectroscopy. *ChemPhysChem* **2005**, *6*, 120−128.

(28) Robertson, E. G.; Simons, J. P. Getting Into Shape: Conformational and Supramolecular Landscapes in Small Biomolecules and Their Hydrated Clusters. *Phys. Chem. Chem. Phys.* **2001**, *3*, 1−18.

(29) Rijs, A. M.; Kabelac, M.; Abo-Riziq, A.; Hobza, P.; de Vries, M. S. Isolated Gramicidin Peptides Probed by IR Spectroscopy. *ChemPhysChem* **2011**, *12*, 1816−1821.

(30) Jaeqx, S.; Du, W. N.; Meijer, E. J.; Oomens, J.; Rijs, A. M. Conformational Study of Z-Glu-OH and Z-Arg-OH: Dispersion Interactions Versus Conventional Hydrogen Bonding. *J. Phys. Chem. A* **2013**, *117*, 1216−1227.

(31) Cocinero, E. J.; Çarçabal, P.; Vaden, T. D.; Davis, B. G.; Simons, J. P. Exploring Carbohydrate-Peptide Interactions in the Gas Phase: Structure and Selectivity in Complexes of Pyranosides with N-Acetylphenylalanine Methylamide. *J. Am. Chem. Soc.* **2011**, *133*, 4548−4557.
(32) Simons, J. P.; Davis, B. G.; Cocinero, E. J.; Gamblin, D. P.; Stanca-Kaposta, E. C. Conformational Change and Selectivity in Explicitly Hydrated Carbohydrates. *Tetrahedron: Asymmetry* **2009**, *20*, 718−722.
(33) Cocinero, E. J.; Stanca-Kaposta, E. C.; Gamblin, D. P.; Davis, B. G.; Simons, J. P. Peptide Secondary Structures in the Gas Phase: Consensus Motif of N-Linked Glycoproteins. *J. Am. Chem. Soc.* **2009**, *131*, 1282−1287.
(34) Cocinero, E. J.; Stanca-Kaposta, E. C.; Dethlefsen, M.; Liu, B.; Gamblin, D. P.; Davis, B. G.; Simons, J. P. Hydration of Sugars in the Gas Phase: Regioselectivity and Conformational in N-Acetyl Glucosamine and Glucose. *Chem.—Eur. J.* **2009**, *15*, 13427−13434.
(35) Simons, J. P.; Stanca-Kaposta, E. C.; Cocinero, E. J.; Liu, B.; Davis, B. G.; Gamblin, D. P.; Kroemer, R. T. Probing The Glycosidic Linkage: Secondary Structures in the Gas Phase. *Phys. Scr.* **2008**, *78*, 058124.
(36) Casaes, R. N.; Paul, J. B.; McLaughlin, R. P.; Saykally, R. J.; Van Mourik, T. Infrared Cavity Ringdown Spectroscopy of Jet-Cooled Nucleotide Base Clusters and Water Complexes. *J. Phys. Chem. A* **2004**, *108*, 10989−10996.
(37) Liu, K.; Fellers, R. S.; Viant, M. R.; McLaughlin, R. P.; Brown, M. G.; Saykally, R. J. A Long Path Length Pulsed Slit Valve Appropriate For High Temperature Operation: Infrared Spectroscopy of Jet-Cooled Large Water Clusters and Nucleotide Bases. *Rev. Sci. Instrum.* **1996**, *67*, 410−416.
(38) Plutzer, C.; Hunig, I.; Kleinermanns, K.; Nir, E.; de Vries, M. Pairing of Isolated Nucleobases: Double Resonance Laser Spectroscopy of Adenine-Thymine. *ChemPhysChem* **2003**, *4*, 838−842.
(39) Nir, E.; Janzen, C.; Imhof, P.; Kleinermanns, K.; de Vries, M. S. Pairing of the Nucleobases Guanine and Cytosine in The Gas Phase Studied by IR-UV Double-Resonance Spectroscopy and Ab Initio Calculations. *Phys. Chem. Chem. Phys.* **2002**, *4*, 732−739.
(40) Nir, E.; Janzen, C.; Imhof, P.; Kleinermanns, K.; de Vries, M. S. Pairing of the Nucleobase Guanine Studied by IR-UV Double-Resonance Spectroscopy and Ab Initio Calculations. *Phys. Chem. Chem. Phys.* **2002**, *4*, 740−750.
(41) van Zundert, G. C. P.; Jaeqx, S.; Berden, G.; Bakker, J. M.; Kleinermanns, K.; Oomens, J.; Rijs, A. M. IR Spectroscopy of Isolated Neutral and Protonated Adenine and 9-Methyladenine. *ChemPhysChem* **2011**, *12*, 1921−1927.
(42) Aguado, E.; León, I.; Cocinero, E. J.; Lesarri, A.; Fernández, J. A.; Castaño, F. Molecular Recognition in the Gas Phase: Benzocaine-Phenol as a Model of Anaesthetic-Receptor Interaction. *Phys. Chem. Chem. Phys.* **2009**, *11*, 11608−11616.
(43) León, I.; Cocinero, E.; Millán, J.; Jaeqx, S.; Rijs, A.; Lesarri, A.; Castaño, F.; Fernández, J. A. Exploring Microsolvation of the Anesthetics Propofol. *Phys. Chem. Chem. Phys.* **2012**, *14*, 4398.
(44) León, I.; Cocinero, E. J.; Millán, J.; Rijs, A. M.; Usabiaga, I.; Lesarri, A.; Castaño, F.; Fernández, J. A. A Combined Spectroscopic and Theoretical Study of Propofol·$(H_2O)_3$. *J. Chem. Phys.* **2012**, *137*, 074303.
(45) León, I.; Millan, J.; Cocinero, E.; Lesarri, A.; Castaño, F.; Fernández, J. A. Mimicking Anaesthetic-Receptor Interaction: a Combined Spectroscopic and Computational study of Propofol···Phenol. *Phys. Chem. Chem. Phys.* **2012**, *14*, 8956−8963.
(46) León, I.; Cocinero, E. J.; Lesarri, A.; Castaño, F.; Fernández, J. A. A Spectroscopic Approach to the Solvation of Anesthetics in Jets: Propofol$(H_2O)_n$, n=4−6. *J. Phys. Chem. A* **2012**, *116*, 8934−8941.
(47) León, I.; Millán, J.; Castaño, F.; Fernández, J. A. A Spectroscopic and Computational Study of Propofol Dimers and Their Hydrated Clusters. *Chemphyschem* **2012**, *13* (17), 3819−3826.
(48) Rijs, A. M.; Kay, E. R.; Leigh, D. A.; Buma, W. J. IR Spectroscopy on Jet-Cooled Isolated Two-Station Rotaxanes. *J. Phys. Chem. A* **2011**, *115*, 9669−9675.
(49) Halgren, T. A. MMFF VII. Characterization of MMFF94, MMFF94s, and Other Widely Available Force Fields For Conformational Energies and For Intermolecular-Interaction Energies and Geometries. *J. Comput. Chem.* **1999**, *20*, 730−748.
(50) Halgren, T. A. Merck molecular force field 0.5. Extension of MMFF94 Using Experimental Data, Additional Computational Data, and Empirical Rules. *J. Comput. Chem.* **1996**, *17*, 616−641.
(51) Halgren, T. A.; Bush, B. L. The Merck Molecular Force Field (MMFF94). Extension and Application. *Abstr. Pap. Am. Chem. Soc.* **1996**, *212*, 2-COMP.
(52) Boys, S. F.; Bernardi, F. Calculation of Small Molecular Interactions by Differences of Separate Total Energies - Some Procedures with Reduced Errors. *Mol. Phys.* **1970**, *19*, 553−566.
(53) Frisch, M. J.; Trucks, G. W.; Schlegel, H. B.; Scuseria, G. E.; Robb, M. A.; Cheeseman, J. R.; Scalmani, G.; Barone, V.; Mennucci, B.; Petersson, G. A.; Nakatsuji, H.; Caricato, M.; Li, X.; Hratchian, H. P.; Izmaylov, A. F.; Bloino, J.; Zheng, G.; Sonnenberg, J. L.; Hada, M.; Ehara, M.; Toyota, K.; Fukuda, R.; Hasegawa, J.; Ishida, M.; Nakajima, T.; Honda, Y.; Kitao, O.; Nakai, H.; Vreven, T.; Montgomery, J. A., Jr.; Peralta, J. E.; Ogliaro, F.; Bearpark, M.; Heyd, J. J.; Brothers, E.; Kudin, K. N.; Staroverov, V. N.; Kobayashi, R.; Normand, J.; Raghavachari, K.; Rendell, A.; Burant, J. C.; Iyengar, S. S.; Tomasi, J.; Cossi, M.; Rega, N.; Millam, J. M.; Klene, M.; Knox, J. E.; Cross, J. B.; Bakken, V.; Adamo, C.; Jaramillo, J.; Gomperts, R.; Stratmann, R. E.; Yazyev, O.; Austin, A. J.; Cammi, R.; Pomelli, C.; Ochterski, J. W.; Martin, R. L.; Morokuma, K.; Zakrzewski, V. G.; Voth, G. A.; Salvador, P.; Dannenberg, J. J.; Dapprich, S.; Daniels, A. D.; Farkas, O.; Foresman, J. B.; Ortiz, J. V.; Cioslowski, J.; Fox, D. J. *Gaussian 09*, revision A02; Gaussian, Inc.: Wallingford, CT, 2009.
(54) Longarte, A.; Fernández, J. A.; Unamuno, I.; Castaño, F. Structure and Ground and First Electronic Excited State Vibrational Modes of the Ethyl-P-Aminobenzoate Conformers. *Chem. Phys.* **2000**, *260*, 83−93.
(55) Howells, B. D.; McCombie, J.; Palmer, T. F.; Simons, J. P.; Walters, A. Laser-Induced Fluorescence Spectroscopy and Structure of Microsolvated Molecular Clusters. Part 2.-Laser-Induced Fluorescence Spectroscopy of Jet-Cooled Ethyl 4-Aminobenzoate, Methyl 4-Aminobenzoate, 4-Aminobenzonitrile and Their Dimethylamino And Pyrrolidino Derivatives. *J. Chem. Soc., Faraday Trans.* **1992**, *88*, 2595−2601.
(56) Aguado, E.; Longarte, A.; Alejandro, E.; Fernández, J. A.; Castaño, F. ZEKE-PFI Spectroscopy of Benzocaine. *J. Phys. Chem. A* **2006**, *110*, 6010−6015.
(57) Fernández, J. A.; Longarte, A.; Unamuno, I.; Castaño, F. A Theoretical and Experimental Study Of The Ethyl-p-Aminobenzoate $(H2O)_n$ (n=1−4) Complexes. *J. Chem. Phys.* **2000**, *113*, 8531−8540.
(58) Hobza, P.; Muller-Dethlefs, K. *Non-Covalent Interactions*; RCS Publishing: Cambridge, 2010.
(59) Thut, M.; Tanner, C.; Steinlin, A.; Leutwyler, S. Time-Dependent Density Functional Theory As a Tool For Isomer Assignments of Hydrogen-Bonded Solute.Solvent Clusters. *J. Phys. Chem. A* **2008**, *112*, 5566−5572.
(60) Biswal, H. S.; Gloaguen, E.; Mons, M.; Bhattacharyya, S.; Shirhatti, P. R.; Wategaonkar, S. Structure of the Indole-Benzene Dimer Revisited. *J. Phys. Chem. A* **2011**, *115*, 9485−9492.
(61) Kumar, S.; Biswas, P.; Kaul, I.; Das, A. Competition Between Hydrogen Bonding and Dispersion Interactions in the Indole···Pyridine Dimer And $Indole_2$···Pyridine Trimer Studied in a Supersonic Jet. *J. Phys. Chem. A* **2011**, *115*, 7461−7472.
(62) Schiccheri, N.; Pasquini, M.; Piani, G.; Pietraperzia, G.; Becucci, M.; Biczysko, M.; Bloino, J.; Barone, V. Integrated Experimental and Computational Spectroscopy Study on Pi-Stacking Interaction: The Anisole Dimer. *Phys. Chem. Chem. Phys.* **2010**, *12*, 13547−13554.